Kid-1 expression is high in differentiated renal proximal tubule cells and suppressed in cyst epithelia

RALPH WITZGALL,[1] NICHOLAS OBERMÜLLER,[2] ULRIKE BÖLITZ,[1]
JAMES P. CALVET,[3] BENJAMIN D. COWLEY, JR.,[3] CHERYL WALKER,[4]
WILHELM KRIZ,[1] NORBERT GRETZ,[2] AND JOSEPH V. BONVENTRE[5]
[1]*Institute of Anatomy and Cell Biology I, University of Heidelberg, 69120 Heidelberg;*
[2]*Medical Research Center, Klinikum Mannheim, University of Heidelberg, 68167 Mannheim, Germany;* [3]*Kansas University Medical Center, Kansas City, Kansas 66160;* [4]*University of Texas M. D. Anderson Cancer Center, Smithville, Texas 78957; and* [5]*Renal Unit and Department of Medicine, Massachusetts General Hospital and Harvard Medical School, Charlestown, Massachusetts 02129*

Witzgall, Ralph, Nicholas Obermüller, Ulrike Bölitz, James P. Calvet, Benjamin D. Cowley, Jr., Cheryl Walker, Wilhelm Kriz, Norbert Gretz, and Joseph V. Bonventre. Kid-1 expression is high in differentiated renal proximal tubule cells and suppressed in cyst epithelia. *Am. J. Physiol.* 275 (*Renal Physiol.* 44): F928–F937, 1998.—The cDNA coding for the transcriptional repressor protein Kid-1 was cloned in a screen for zinc finger proteins, which are regulated during renal development and after renal ischemia. Kid-1 mRNA levels increase in the course of postnatal renal development and decrease after acute renal injury caused by ischemia or administration of folic acid. We have raised a monoclonal anti-Kid-1 antibody and demonstrate that the Kid-1 protein is strongly expressed in the proximal tubule of the adult rat kidney. During nephron development, the Kid-1 protein appears after the S-shaped body stage concomitantly with the brush-border enzyme alkaline phosphatase. In two animal models of polycystic kidney disease, the expression of Kid-1 is downregulated. The loss of expression of Kid-1 in cyst wall cells correlates with the loss of alkaline phosphatase histochemical staining. Kid-1 mRNA levels are also reduced in rodent renal cell carcinomas, another condition characterized by epithelial cell dedifferentiation and increased proliferation. We propose that Kid-1 plays an important role during the differentiation of the proximal tubule.

renal development; renal cell carcinoma; polycystic kidney disease; gene regulation; transcriptional repression

THE MORPHOLOGICAL PROCESSES leading to the formation of the fully differentiated kidney have been well described (29), whereas the cellular and molecular events responsible for the ordered pattern of renal development are poorly understood. Gene targeting experiments have revealed that transcription factors play critical roles at different stages of nephrogenesis, and it can therefore be assumed that a hierarchy of genetic regulation exists. Inactivation of the *WT*-1 (21), *Pax*-2 (34), and *Emx*-2 (24) genes leads to renal agenesis, indicating that the proteins encoded by these genes act at a very early stage of renal development. When the *BF*-2 gene is inactivated, renal tissue is present but the number of nephrons that develop totals only ~10% of the number present in normal mouse kidneys (16), suggesting that BF-2 controls genes necessary at a stage of metanephrogenesis later than the stages in which WT-1, Pax-2, and Emx-2 are critical. The protein encoded by the hepatocyte nuclear factor (*HNF*)-1 gene appears to play a role at a very late stage of nephron development, since the inactivation of the *HNF*-1 gene leads to defects specifically in the proximal tubule (27).

We have cloned a rat cDNA encoding a zinc finger protein that we named Kid-1 [predominantly found in the kidney ("k"), suppressed after renal ischemia ("i"), and appearing late in renal development ("d")] (38). The mRNA for Kid-1 is barely detectable at the time of birth in the rat kidney, but levels increase after birth and reach the highest levels in the adult kidney (38). After ischemic or toxic injury to the adult kidney, at a time when many kidney cells dedifferentiate and undergo mitosis, Kid-1 mRNA levels decline to a degree comparable to that in the newborn kidney (38). Northern blot and RT-PCR analysis of a variety of rat organs have shown that among all the organs tested, the Kid-1 mRNA is predominantly expressed in the kidney (38). This result was subsequently confirmed in the mouse (3), where in addition comparable Kid-1 mRNA levels could also be detected in the eye (expression of Kid-1 mRNA in the eye was not analyzed in the rat). A molecular analysis of the Kid-1 protein led to the finding that the non-zinc finger region of Kid-1 was able to confer transcriptional repressor activity (38). More specifically, the transcriptional repressor activity of Kid-1 is conferred by the Krüppel-associated box (KRAB)-domain at the NH_2-terminal of the protein, a widely distributed motif among Cys_2His_2-zinc finger proteins (23, 39).

To learn more about the potential role of Kid-1 in the kidney, we evaluated the expression of Kid-1 during nephron development, in two models of polycystic kidney disease and in rat renal cell carcinomas. Polycystic kidney disease and renal cell carcinomas are two conditions in the adult kidney that are characterized by an increased rate of epithelial cell proliferation and a loss of differentiation (4). One of the polycystic kidney disease models investigated was the C57BL/6J (*cpk*/*cpk*) mouse, a model with an autosomal recessive pattern of inheritance (12, 13, 28); the other model was the Han:SPRD (*cy*/+) rat, a model with an autosomal dominant pattern of inheritance (9, 30). In addition, to

The costs of publication of this article were defrayed in part by the payment of page charges. The article must therefore be hereby marked "*advertisement*" in accordance with 18 U.S.C. Section 1734 solely to indicate this fact.

further test our hypothesis that Kid-1 expression is suppressed in dedifferentiated epithelia, we examined the expression pattern of Kid-1 in the Eker rat model of hereditary renal cell carcinoma (11) and in transformed rat kidney epithelial cell lines (35). Our results indicate that the expression of the Kid-1 protein is induced at a late stage of differentiation of the proximal tubule and that it is downregulated in cyst wall cells of polycystic kidneys and in renal cells tumors. This downregulation is likely related to the dedifferentiated state of these cells. Kid-1 may control genes important for the abnormal phenotype in polycystic disease.

MATERIALS AND METHODS

Preparation of a monoclonal anti-Kid-1 antibody. A fragment coding for amino acids 72–173 of the rat Kid-1 protein was subcloned into the plasmid pET-21b (Novagen, Madison, WI). The resulting plasmid, pET-21b/Kid-1, was used to express a fragment of the rat Kid-1 protein without the highly conserved KRAB and zinc finger domains in *Escherichia coli*. Because the recombinant protein contained a tail of six histidine residues at its COOH terminal, it could easily be purified over a Ni^{2+} column according to the manufacturer's instructions (Novagen). Approximately 75 μg of the purified protein was injected subcutaneously into BALB/c mice in 3-wk intervals. After four injections, splenic lymphocytes were harvested and hybridomas were prepared according to standard protocols (1). Culture supernatants were assayed on a dot blot with purified glutathione *S*-transferase (GST)/Kid-1 fusion protein. Supernatants yielding a positive signal in the dot blot assay were further tested in a Western blot. To obtain a clonal population of cells, hybridomas were subcloned by limiting dilution in a 96-well plate.

Hybridoma cell culture supernatants were combined with saturated $(NH_4)_2SO_4$ in a ratio of 55:45 (vol:vol). After an incubation of 2–4 h at 4°C, the antibody suspension was centrifuged 20 min at 4°C and 12,000 *g*. The antibody pellet was dissolved in PBS ($\frac{1}{100}$ of the original cell culture volume) and then dialyzed against PBS (1).

Epitope mapping. Rat Kid-1 cDNA fragments coding for amino acids 81–195 (region between the KRAB domain and the zinc finger domain), amino acids 1–195 (Kid-1 without the zinc finger domain), amino acids 53–576 (Kid-1 without the KRAB-A domain), and amino acids 174–576 (zinc finger domain only) were subcloned into the plasmid pGEX-KG (15), which resulted in the expression of fusion proteins with GST in *E. coli*. Equal amounts of bacterial extracts were run on SDS-PAGE gels and either stained with Coomassie brilliant blue or subjected to Western blot analysis.

Transient transfection of COS-7 cells. The cDNA coding for the full-length Kid-1 protein was subcloned into the mammalian expression vector pMT3 [pMT2 (18) modified to encode the nine-amino acid hemagglutinin (HA) epitope tag of the influenza virus at the NH_2 terminal of the insert]; transcription is driven by the adenovirus major late promoter. COS-7 cells were grown in Dulbecco's minimal essential medium supplemented with 10% calf serum. One day before transfection, cells were plated at a density of $2.5–4 \times 10^5$ cells per 100-mm dish. For transfection, cells were exposed to 20 μg of DNA in 5 ml of Dulbecco's minimal essential medium-400 μg/ml DEAE-dextran (Sigma, Deisenhofen, Germany)-0.1 mM chloroquine (Sigma). Three hours after the addition of DNA, the medium was removed and the cells were shocked for 2 min at room temperature with 10% dimethyl sulfoxide (Sigma) in 1× PBS. After the shock treatment, the cells were washed once with PBS and new medium was added. Cells were harvested at the indicated times after transfection.

Preparation of nuclear extracts. Nuclear extracts were prepared as described by Hoppe-Seyler et al. (17). Two to three days after transfection, COS-7 cells were washed twice with PBS and scraped into a microcentrifuge tube. The cells were centrifuged for 5 min at 1,250 *g*, and the pellet was resuspended in lysis buffer (150 mM NaCl; 10 mM Tris, pH 7.9; 1 mM EDTA, pH 8.0; 0.6% Nonidet P-40). After an incubation of 5 min on ice, the cells were centrifuged 5 min at 1,250 *g*. The supernatant (corresponding to the cytoplasmic fraction) was saved, and the nuclear pellet was resuspended in nuclear extract buffer [1.5 mM $MgCl_2$; 10 mM HEPES, pH 7.9; 0.1 mM EGTA; 0.1 mM EDTA; 0.5 mM dithiothreitol (DTT); 0.5 mM phenylmethylsulfonyl fluoride; 25% glycerol; 420 mM NaCl]. The nuclear suspension was incubated 20 min on ice and then centrifuged 5 min at 14,000 *g*. The supernatant (corresponding to the soluble nuclear fraction) was saved, and the remaining pellet was solubilized by sonication in PBS-6 M urea.

Immunocytochemistry of kidney sections. Adult Sprague-Dawley rats (70–100 days old) were anesthetized with pentobarbital sodium (6.5 mg/100 g body wt). Anesthetized rats were perfused retrogradely through the aorta for 3 min each with PBS-2% paraformaldehyde and subsequently with PBS-18% sucrose at a pressure of 200–220 mmHg. Newborn Sprague-Dawley rats were anesthetized with ether and perfused with PBS-2% paraformaldehyde through the left ventricle at a pressure of 180–200 mmHg, before the kidneys were removed and immersed for 2 h in PBS-18% sucrose. Kidneys were snap-frozen in isopentane cooled with liquid nitrogen and stored at −80°C until further use. Kidneys were sectioned at 6- to 8-μm thickness, air-dried for 30 min, and blocked for 2 h at room temperature in PBS-2% BSA-0.1% Triton X-100. The $(NH_4)_2SO_4$-precipitated anti-Kid-1 antibody 5D12 was applied at a dilution of 1:50–1:100 in PBS-2% BSA, after which the section was first incubated for 2 h at room temperature before being stored overnight at 4°C. The next morning, sections were washed three times with PBS and incubated 1 h at room temperature with the secondary antibody [Cy3-coupled rat anti-mouse IgG from Dianova (Hamburg, Germany) diluted 1:300]. The sections were washed again three times with PBS and then mounted. When necessary, nuclei were stained after the third wash by incubating the sections for 3 min in Hoechst stain 33258 (Sigma) at a concentration of 10 μg/ml.

Double-labeling was performed with a sheep anti-human Tamm-Horsfall protein antibody (diluted 1:200; Biotrend, Köln, Germany), which was applied simultaneously with the murine monoclonal anti-Kid-1 antibody 5D12. The primary antibodies were detected with FITC-conjugated anti-sheep Ig antibody (diluted 1:80; Sigma) and Cy3-conjugated anti-mouse Ig antibody (Dianova). For preabsorption experiments, the primary antibody was incubated 2 h at room temperature with 100 ng of GST or a GST/Kid-1N (GST fused to amino acids 1–195 of the rat Kid-1 protein) fusion protein per 1 μl of antibody solution before being applied to the tissue section.

Alkaline phosphatase histochemistry. After incubation with the secondary antibody and the ensuing three washes, the sections were incubated 15 min at room temperature (or until an appropriate color development occurred) in 0.3 mM nitro blue tetrazolium chloride and 0.3 mM 5-bromo-4-chloro-3-indolyl phosphate (4-toluidine salt) in 0.2 M Tris·HCl buffer, pH 9.5. The reaction was stopped by immersing the sections for 10 min in distilled water, after which the sections were fixed again in 4% paraformaldehyde (in PBS) for 10 min, rinsed in water, and mounted.

Animal models of polycystic kidney disease and Eker rat model of hereditary renal cell carcinoma. The Han:SPRD (*cy*/+) rat, a model for autosomal dominant polycystic kidney disease (PKD) (9, 30); the C57BL/6J (*cpk*/*cpk*) mouse, a model for autosomal recessive PKD (12, 13, 28); and the Eker rat model of hereditary renal cell carcinoma (11, 36) have been characterized in detail in previous reports. Animals were maintained as inbred colonies in the University of Kansas Medical Center Animal Care Facility [Han:SPRD (*cy*/+) rats and C57BL/6J (*cpk*/*cpk*) mice], the Animal Care Facility of the Medical Research Center in Mannheim [Han:SPRD (*cy*/+) rats], or the Chemical Industry Institute of Toxicology in Research Triangle Park, NC (Eker rats).

Cell culture. Transformed rat kidney epithelial (TRKE) cell lines were established and characterized as described previously (19, 35). In brief, immortal rat kidney epithelial cell lines were created by exposure of primary cultures to the chemical mutagen *N*-methyl-*N'*-nitro-*N*-nitrosoguanidine. TRKE-8, in addition to being immortalized, forms adenocarcinomas in nude mice. Cell lines TRKE-4, TRKE-5, TRKE-7, and TRKE-8 were used in the experiments described in this report. Cells were harvested either at logarithmic growth or after having reached confluency.

Preparation of RNA. By use of a modification of the technique of Chomczynski and Sacchi (6), RNA was isolated from right kidneys of Han:SPRD rats as previously described (8, 9). Briefly, right kidneys were homogenized in GTC solution (4 M guanidine thiocyanate, 25 mM trisodium citrate, 0.1 M β-mercaptoethanol, 0.1% antifoam A, pH 7.0) using a Polytron tissue homogenizer. GTC homogenates were treated by sequential addition of 2 M sodium acetate (pH 4), phenol, and chloroform with vortexing after each addition. After centrifugation, the aqueous layer was transferred to a fresh tube, and RNA was precipitated with isopropanol. RNA was pelleted by centrifugation, redissolved, chloroform extracted, and ethanol precipitated. RNA was again pelleted by centrifugation, redissolved, and quantitated by spectrophotometry. After a final ethanol precipitation, RNA was stored at −20°C until use.

Generation of ^{32}P-labeled DNA probes. Human full-length glyceraldehyde-3-phosphate dehydrogenase (a gift of M. Alexander-Bridges, Massachusetts General Hospital) was random primed according to standard protocols (1). Unincorporated nucleotides were removed by running the reaction over a spin column (Bio-Rad, Hercules, CA).

Radiolabeled single-stranded antisense DNA was prepared as described by Sturzl and Roth (33). PCR buffer (final concentration 50 mM KCl; 10 mM Tris·HCl, pH 8.4; 2.5 mM $MgCl_2$); 250 μM dATP, dGTP, and dTTP; 6.3 μM dCTP; 5 μl α-^{32}P-dCTP (10 μCi/μl, 3,000 Ci/mmol); 250 ng primer; 2 U AmpliTaq polymerase; and 200 ng linearized template pBlue/Kid-1(−) (containing nucleotides 1–897 of the rat Kid-1 cDNA) (38) were combined in a total volume of 10 μl. Fifty microliters of mineral oil was added to each reaction tube. After 40 cycles of 30 s at 95°C, 1 min at 50°C, 2 min at 72°C, and a final extension of 10 min at 72°C, unincorporated nucleotides were removed over a spin column (Bio-Rad).

Northern blot and hybridization. RNA samples were run on agarose gels and blotted onto Nylon membranes according to standard protocols (1). Blots were prehybridized in 2× SDE (10× SDE is 1 M NaCl; 500 mM sodium phosphate, pH 7.0; 25 mM EDTA), 5% SDS, 100 μg/ml yeast tRNA, and 100 μg/ml denatured salmon sperm DNA at 55°C for 5 h (38). Then, 2.5×10^5 cpm of random-primed or single-stranded DNA probe per milliliter of hybridization buffer was added, and the hybridization was continued overnight at the same temperature. The following morning, the blots were washed three times for 15 min each at room temperature with 2× SSC, two times for 10 min each at 65°C with 2× SSC, and two times for 5 min each at 65°C with 0.1× SSC (this last wash was carried out only when probe and RNA were from the same species).

RNase protection assay. T3/T7 buffer (final concentrations: 20 mM Tris·HCl, pH 7.5; 3 mM $MgCl_2$; 5 mM DTT; 2 mM spermidine); 400 μM ATP, GTP, and UTP; 40 U RNasin; 10 μl of α-^{32}P-CTP (10 μCi/μl); 0.5 μg of linearized template Z5.9zf(−) (containing nucleotides 552–897 of the rat Kid-1 cDNA) (38); and 10 U of T3 or T7 RNA polymerase were combined in a total volume of 20 μl. After 60 min at 37°C, 2 μl of 10 mg/ml tRNA and 10 U of DNase I (RNase free) were added, and the incubation continued for 15 min at 37°C. Unincorporated nucleotides were removed over a spin column. The RNA probe was precipitated in the presence of ethanol, and the pellet was dissolved in 4:1 (vol:vol) formamide:hybridization mix (final concentration 40 mM PIPES, pH 6.4; 400 mM NaCl; 1 mM EDTA) to achieve a probe concentration of 1.5×10^4 cpm/μl. Lyophilized sample RNA was brought up in 30 μl of probe RNA and denatured 5 min at 85°C. Hybridization was carried out overnight at 45°C. The next morning, 350 μl RNase digestion buffer (10 mM Tris·HCl, pH 7.5; 300 mM NaCl; 5 mM EDTA; 40 μg/ml RNase A, 2 μg/ml RNase T1) were added and free probe digested for 45 min at 30°C. RNase was inactivated by incubating for 15 min at 37°C after addition of 10 μl of 20% SDS and 5 μl of 10 mg/ml proteinase K. Finally, the reaction was phenolized and the supernatant was ethanol precipitated and analyzed on a sequencing gel (1).

RESULTS

Characterization of the monoclonal anti-rat Kid-1 antibody 5D12. To characterize the endogenous Kid-1 protein, we generated a monoclonal antibody by immunizing BALB/c mice with a recombinant rat Kid-1 peptide (amino acids 72–173), lacking the highly conserved KRAB and zinc finger domains, to minimize the possibility of cross-reactivity of an anti-Kid-1 antibody with other zinc finger proteins. One hybridoma, 5D12, produced an antibody of the IgG1-κ class that was tested on a Western blot with various bacterially expressed GST/Kid-1 fusion proteins (Fig. 1, *A* and *C*). Whereas proteins containing amino acids 53–195 were recognized by the 5D12 antibody (Fig. 1*B*, *lanes 4* and *5*), a peptide containing amino acids 81–195 was not (Fig. 1*B*, *lane 3*). GST alone or the zinc finger domain of Kid-1 did not react with the antibody (Fig. 1*B*, *lanes 2* and *6*, respectively). This detection pattern demonstrates the specificity of the anti-Kid-1 antibody. Since the peptide used to generate the antibody included only amino acids 72–173, the amino acids recognized by the antibody 5D12 likely include those at position 72–81 of Kid-1.

The 5D12 antibody was further characterized using COS-7 cells transiently transfected with an HA epitope-tagged, full-length Kid-1 protein. Two days after transfection, the cells were harvested and lysed with nonionic detergent, and nuclear extracts were prepared by a protocol using 420 mM NaCl. Western blot analysis with the 5D12 monoclonal anti-Kid-1 antibody yielded a single band in the pellet fraction remaining after the

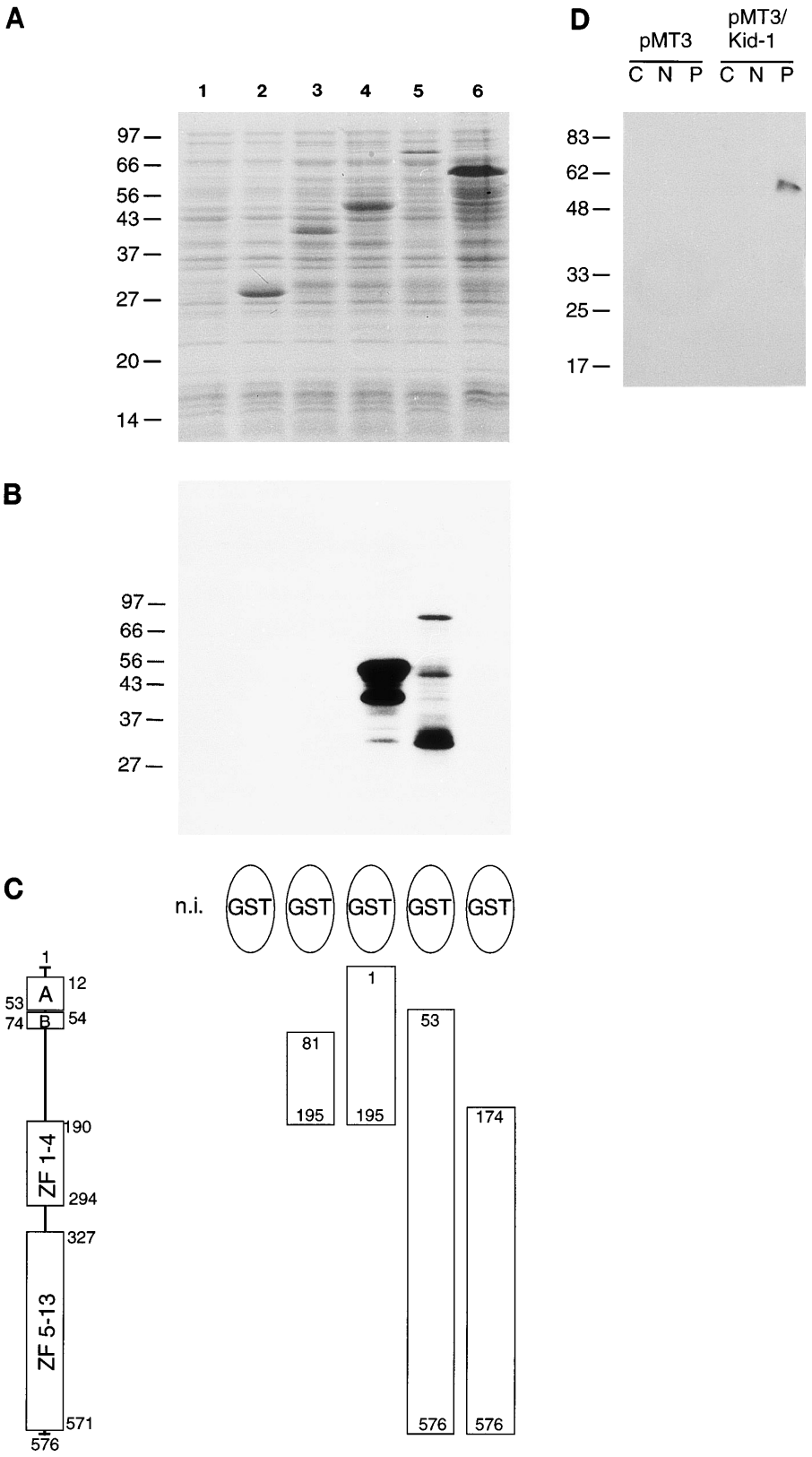

Fig. 1. Specificity of the anti-Kid-1 antibody 5D12. Fusion proteins between glutathione *S*-transferase (GST) and various portions of Kid-1 (*A* shows bacterial extracts with different fusion proteins on a Coomassie-stained gel; *C* describes the various constructs aligned with the domain structure of Kid-1) were tested on a Western blot for their reactivity with the anti-Kid-1 antibody 5D12. Only 2 of the fusion proteins reacted with antibody 5D12 (*B*), attesting to the specificity of the antibody and narrowing down the epitope that is recognized by this monoclonal antibody to a region close to the Krüppel-associated box (KRAB)-B domain between amino acids 53 and 81 (molecular weight markers shown at *left*). Multiple bands seen with both constructs on the Western blot probably correspond to partially degraded Kid-1 fusion proteins. In COS-7 cells transiently expressing Kid-1, only a single band can be detected in the insoluble nuclear pellet fraction (*D*). ni, Not induced; C, detergent-soluble proteins; N, soluble nuclear proteins; P, insoluble nuclear proteins; ZF, zinc finger encoding region of the cDNA (e.g., ZF1–4 encodes first 4 zinc fingers of Kid-1); A, KRAB-A encoding region; B, KRAB-B encoding region (see Ref. 38).

extraction with 420 mM NaCl, indicating that the Kid-1 protein adhered tightly to as-yet-unidentified nuclear structures (Fig. 1*D*). Mock-transfected cells yielded no signal, again attesting to the specificity of the anti-Kid-1 antibody 5D12.

Expression of the Kid-1 protein in adult and newborn rat kidneys. In a previous report (38), we described the temporal expression pattern of the Kid-1 mRNA during renal development and in the recovery phase after ischemic acute renal failure. Having demonstrated the

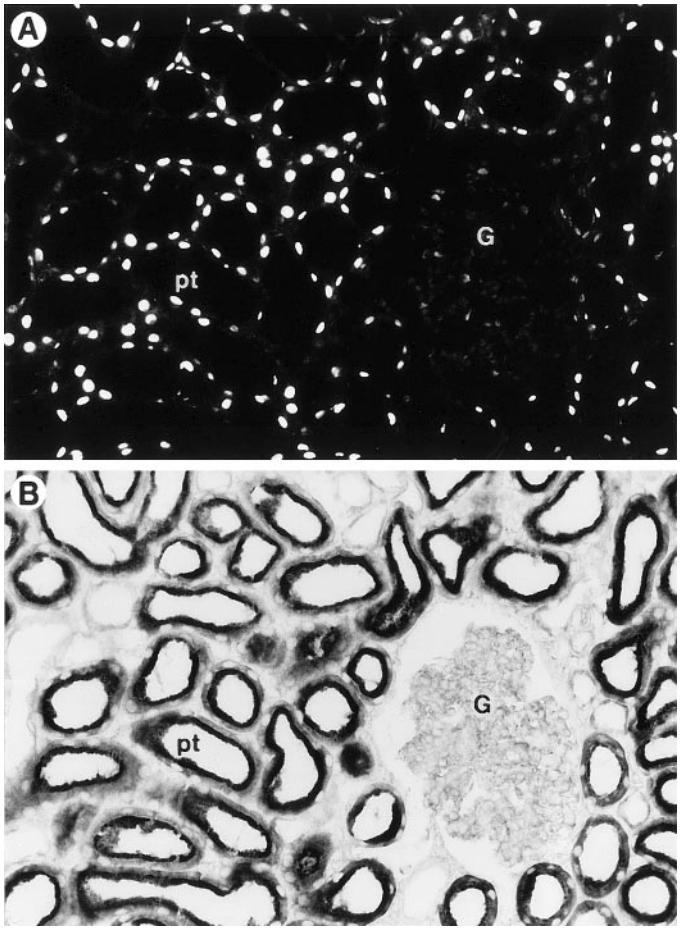

Fig. 2. Immunohistochemical analysis of the expression of Kid-1 in the cortex of adult rat kidneys. Staining of cortical rat kidney sections with the anti-Kid-1 antibody 5D12 resulted in a strong nuclear labeling of many tubular profiles (*A*). These profiles could be identified as proximal tubules by histochemical staining for alkaline phosphatase (*B*). G, glomerulus; pt, proximal tubule. Magnification, ×185.

specificity of the anti-Kid-1 antibody, we then set out to determine the spatial expression pattern of the Kid-1 protein in the rat kidney. Staining of kidney sections from adult rats with the anti-Kid-1 antibody 5D12 resulted in the obvious nuclear staining of tubular profiles in the cortex and the outer stripe of the outer medulla. This nuclear staining could be competed out by preabsorbing the antibody with an excess of a GST/Kid-1 fusion protein, whereas preabsorption with GST alone had no effect (data not shown). To define more precisely which part of the nephron expresses the Kid-1 protein, we performed histochemical staining for alkaline phosphatase, a marker for proximal tubules, on the same tissue section. Tubular profiles with alkaline phosphatase activity also showed a strong expression of the Kid-1 protein, thus demonstrating that Kid-1 is expressed in the S1, S2, and S3 segments of proximal tubules (Figs. 2 and 3). In addition, some faint nuclear staining was seen in tubular profiles not showing alkaline phosphatase activity. Such profiles were identified as thick ascending limbs by staining with an anti-Tamm-Horsfall protein antibody, and as collecting ducts (Fig. 3).

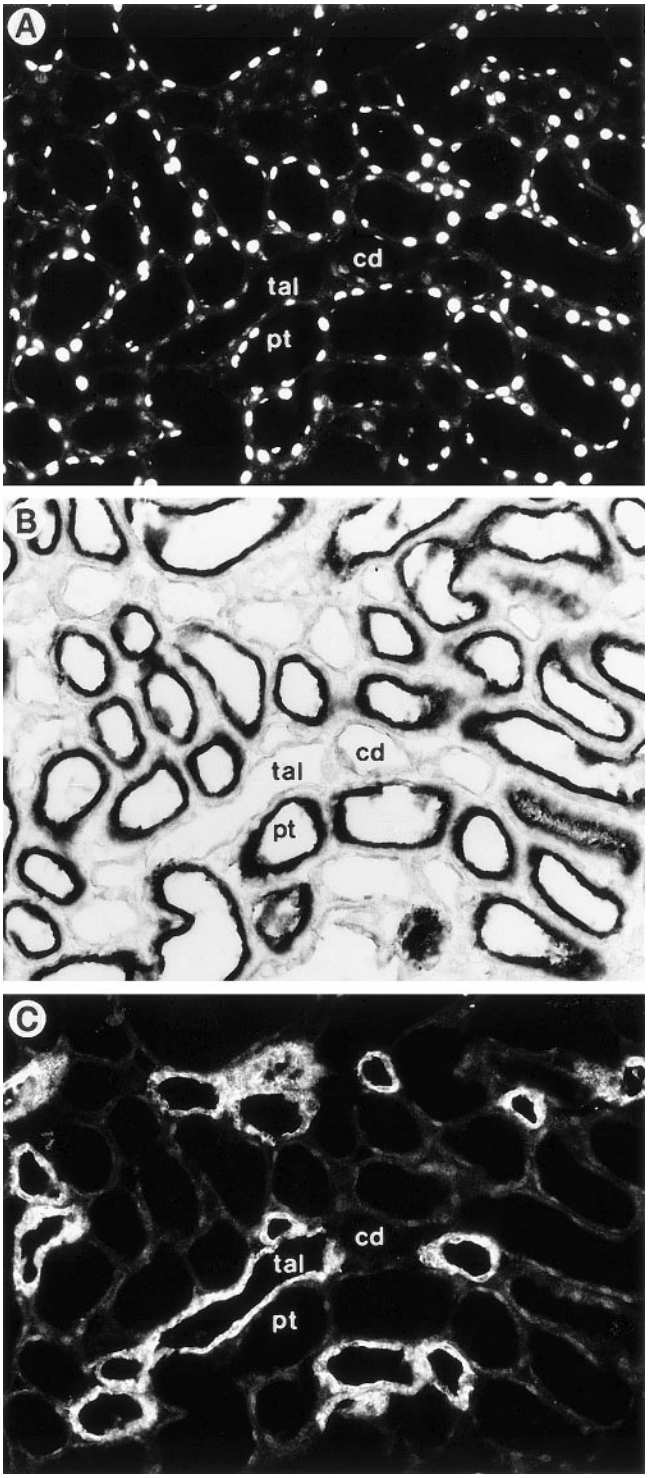

Fig. 3. Immunohistochemical analysis of expression of Kid-1 in the outer stripe of adult rat kidneys. Staining of the outer stripe of adult rat kidneys with the anti-Kid-1 antibody 5D12 shows prominent nuclear staining in the S3 segment of the proximal tubule (*A*), as demonstrated by simultaneous histochemical staining for alkaline phosphatase activity (*B*). There was faint nuclear staining in collecting ducts and thick ascending limbs. The identity of the thick ascending limbs was confirmed by the simultaneous application of an anti-Tamm-Horsfall protein antibody (*C*). pt, Proximal tubule; tal, thick ascending limb; cd, collecting duct. Magnification, ×190.

At time of birth, the rat kidney is not completely developed, containing a rim of metanephrogenic mesenchyme immediately beneath the capsule and early metanephrogenic forms such as comma- and S-shaped bodies deeper toward the medulla (22). In the kidney of the newborn rat only background staining could be detected with the anti-Kid-1 antibody below the capsule, whereas there was a more pronounced nuclear staining toward the medulla, which suggested that the Kid-1 protein was expressed in the tubule at latter stages of nephron development (Fig. 4*A*). Alkaline phosphatase activity has been described to increase progressively during postnatal renal development and can therefore serve as a marker for the differentiation state of proximal tubules (5). The histochemical appearance of alkaline phosphatase activity (Fig. 4*B*) and Kid-1 immunoreactivity (Fig. 4*A*) correlated well, indicating that the expression of the Kid-1 protein occurred in the late stages of differentiation of the proximal tubule. Comparison of immunohistochemical staining for Kid-1 (Fig. 4*A*) and hematoxylin and eosin staining (Fig. 4*C*) on the same section demonstrated that other structures, such as the ureter stem, reacted only weakly and the ureteric bud, the condensed mesenchyme, and comma- and S-shaped bodies did not react at all with the anti-Kid-1 antibody.

Expression of Kid-1 mRNA and protein in polycystic kidneys from rat and mouse. The Han:SPRD (*cy*/+) rat is a model for autosomal dominant polycystic kidney disease. The cysts in the Han:SPRD (*cy*/+) rat originate predominantly from the proximal tubule (26). We analyzed the expression of the Kid-1 mRNA and protein in this model of polycystic kidney disease. When polycystic kidneys from 3-, 8-, and 24-wk-old male rats were studied, Kid-1 mRNA levels in kidneys from heterozygous (*cy*/+) rats were lower than those in kidneys from age-matched, wild-type (+/+) controls (Fig. 5). In polycystic kidneys from female Han:SPRD rats, however, no marked difference could be seen between the Kid-1 mRNA levels of heterozygous (*cy*/+) animals and those of wild-type animals at any age (Fig. 5).

These observations were extended by analyzing the distribution of the Kid-1 protein in cyst wall cells of male Han:SPRD (*cy*/+) rats using immunocytochemical staining with the anti-Kid-1 antibody 5D12. Alkaline phosphatase served as a marker for the differentiation state of cyst wall epithelia. Many cyst-lining cells showed no alkaline phosphatase activity, as demonstrated previously (26) (Fig. 6*A*). Staining with the anti-Kid-1 antibody was decreased in the cyst epithelial cells, but was lost completely only in a subpopulation of cyst wall cells (Fig. 6*B*). Thus in many cysts the Kid-1 protein was still present when alkaline phosphatase staining was absent, although in these cyst-lining cells the Kid-1 expression level was decreased relative to cells in noncystic proximal tubules or cyst wall cells that still expressed alkaline phosphatase.

To determine whether our findings were specific to polycystic kidneys of the Han:SPRD (*cy*/+) rat, we also evaluated the expression of Kid-1 mRNA by Northern blot analysis in polycystic kidneys from C57BL/6J (*cpk*/*cpk*) mice, a model for autosomal recessive PKD (Fig. 7). Compared with unaffected (+/+) littermates, the levels of Kid-1 mRNA were markedly decreased,

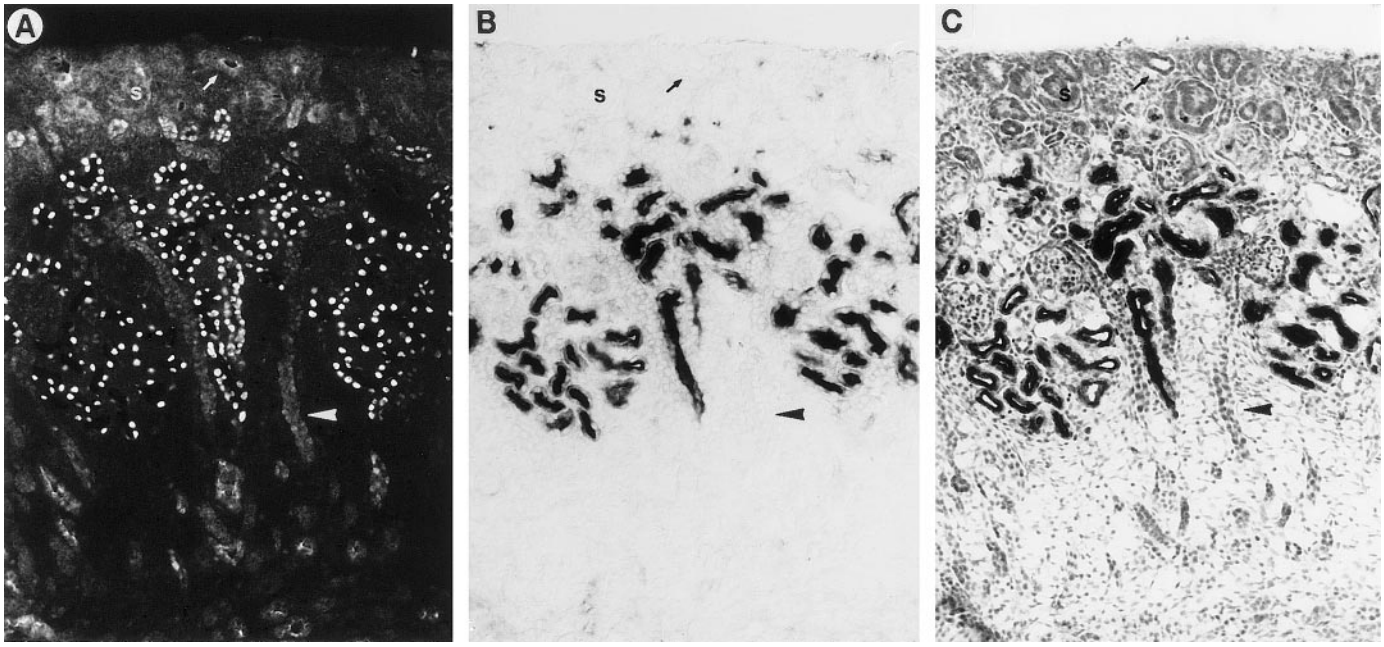

Fig. 4. Expression of Kid-1 in the kidney of the newborn rat. Kidney sections from newborn rats were subjected to immunohistochemistry with the anti-Kid-1 antibody 5D12 (*A*) and to histochemistry for alkaline phosphatase (*B*). To clearly demonstrate the morphology of the various developmental stages, the same section was subsequently stained with hematoxylin and eosin (*C*). Kid-1 is strongly expressed in those profiles, which are also alkaline phosphatase positive, only weakly in the stem of the invading ureter (arrowheads), and not at all in ureteric buds (arrows) and earlier stages of nephron development such as S-shaped bodies (S). Magnification, ×185.

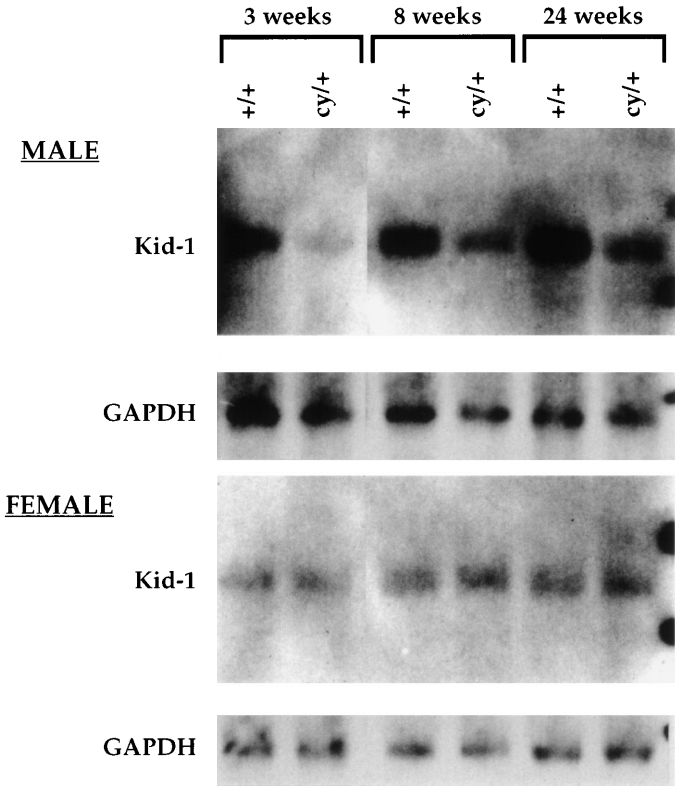

Fig. 5. Kid-1 mRNA levels are low in polycystic kidney disease in the Han:SPRD (*cy*/+) rat. Northern blots with 20 μg of total RNA from Han:SPRD (*cy*/+) and (+/+) rat kidneys were hybridized with PCR-generated single-stranded Kid-1 antisense probe. Random-primed glyceraldehyde-3-phosphate dehydrogenase (GAPDH) cDNA served as control for loading of RNA. Whereas Kid-1 mRNA levels in male Han:SPRD (*cy*/+) rat kidneys were lower than those in kidneys from wild-type (+/+) animals at 3, 8, and 24 wk of age, no difference could be detected at any age when kidneys from female (*cy*/+) animals were compared with those from age-matched, wild-type (+/+) animals.

results similar to our observations in polycystic kidneys from Han:SPRD (*cy*/+) rats.

Expression of Kid-1 mRNA in rat renal cell carcinomas and transformed rat renal epithelial cell lines. If decreased Kid-1 expression is a common feature of the dedifferentiated proximal tubule cell, then one might expect Kid-1 expression to be suppressed in renal cell carcinoma and transformed renal epithelial cell lines, too. The expression of Kid-1 mRNA was examined in three different Eker renal cell carcinomas (Fig. 8). Eker tumors are derived from rats carrying a mutation in the *Tsc*-2 tumor suppressor gene (20, 41), which predisposes them to renal cell carcinomas (11). In all three samples of renal cell carcinomas obtained, the mRNA levels of Kid-1 were lower than in the normal adult kidney tissue taken from the same rat kidney. Kid-1 mRNA levels were also low in several transformed rat kidney epithelial cell lines. Interestingly, the expression level of Kid-1 mRNA in the tumor-forming TRKE-8 cell line was the lowest in the four cell lines examined (Fig. 8). TRKE-8 is the only one of these cell lines found to have deletions in $p15^{INK4B}$ and $p16^{INK4}$, two members of a tumor suppressor cyclin-dependent kinase-4 family (19). No differences were found between cells in

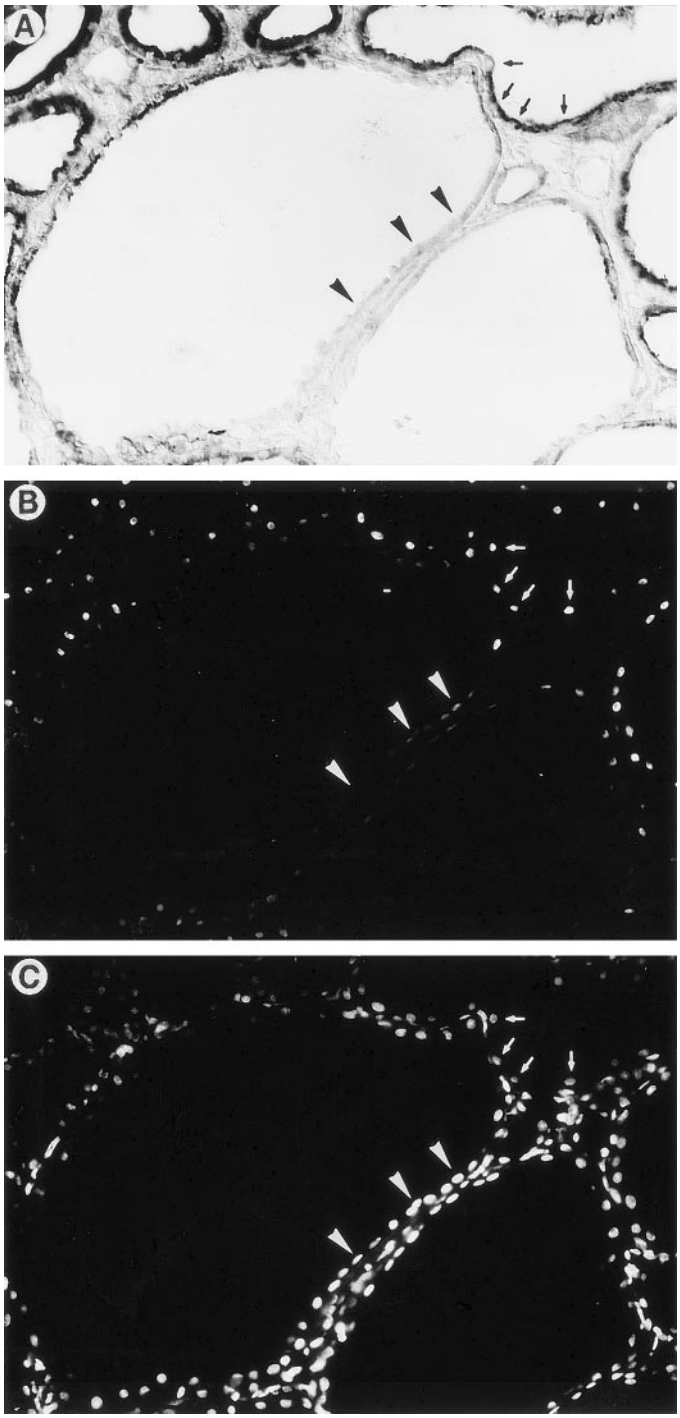

Fig. 6. Expression of the Kid-1 protein in cyst wall cells of a polycystic kidney from a 38-day old male Han:SPRD (*cy*/+) rat. Alkaline phosphatase expression, as demonstrated by histochemistry, is markedly decreased in large cysts, but not in smaller cysts and in noncystic proximal tubule cells (*A*). The Kid-1 protein, detected with the monoclonal anti-Kid-1 antibody 5D12 and subsequent incubation with a Cy3-labeled secondary antibody (*B*), is expressed strongly in nondilated proximal tubules and cysts that still expressed alkaline phosphatase markedly (arrows), but only weakly in cyst wall cells lacking alkaline phosphatase activity (arrowheads). The same section was also stained with the DNA-binding dye Hoechst 33258 to identify nuclei (*C*). Magnification, ×185.

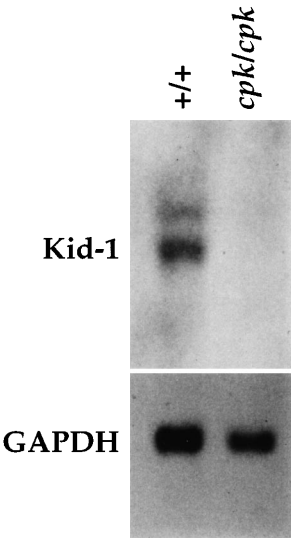

Fig. 7. Kid-1 mRNA is low in advanced stages of polycystic kidney disease in the C57BL/6J (*cpk*/*cpk*) mouse kidney. A Northern blot with 5 μg of poly(A)-selected RNA from kidneys of 3-wk-old C57BL/6J (*cpk*/*cpk*) mice was hybridized with PCR-generated, single-stranded Kid-1 antisense probe. Random-primed GAPDH cDNA served as control for equal loading of RNA. Homozygous (*cpk*/*cpk*) animals express much less Kid-1 mRNA in their kidneys than do their normal (+/+) litter mates.

logarithmic growth and at confluence in any of the cell lines.

DISCUSSION

Expression of Kid-1 in the adult and newborn rat kidney. In the adult rat kidney, the Kid-1 protein is strongly expressed in all segments of the proximal tubule, a localization confirmed by simultaneous histochemical analysis of alkaline phosphatase activity. By the same measure, Kid-1 appears at a relatively advanced stage of nephron development, that is, shortly after the S-shaped body stage at a time when alkaline phosphatase activity is also expressed. Kid-1 is a transcriptional repressor (38), and it can therefore be hypothesized that Kid-1 shuts off genes that are dispensable or even inhibitory for the establishment of the phenotype of the proximal tubule. Alternatively, similar to the hypothesis set forth for the transcriptional repressor REST/neuron-restrictive silencer factor, which is expressed ubiquitously outside the nervous system and shuts off neuron-specific genes (7, 31), Kid-1 may shut off genes that are expressed in other nephron segments, such as the thin limb and distal tubule of the nephron. This expression pattern of Kid-1 is similar to the one described for the transcription factors HNF-1 (27) and AP-2α (25). The HNF-1 protein appears to be necessary for the transcription of certain genes in proximal tubular cells. An inactivation of the *HNF*-1 gene results in a renal Fanconi syndrome caused by a dysfunction of the proximal tubule, because target genes of *HNF*-1 are no longer transcribed at sufficiently high levels (27). Whether Kid-1 is one of those target genes has yet to be evaluated.

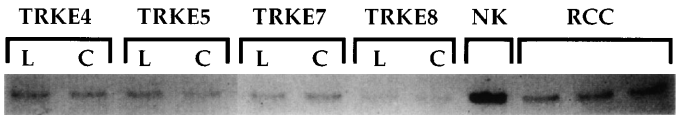

Fig. 8. Expression of Kid-1 in rat Eker renal cell carcinomas (RCC) and transformed epithelial cell lines. Ten micrograms each of total RNA from 1 sample of normal adult rat kidney (NK) and 3 samples of different Eker renal cell carcinomas were analyzed in a RNase protection assay with in vitro-transcribed anti-sense Z5.9zf(−). The protected band is shown in each lane. In all 3 cases of renal cell carcinomas, intensity of the band was considerably lower than in the normal adult rat kidney. RNA from 4 permanent rat kidney epithelial cell lines, TRKE-4, TRKE-5, TRKE-7, and TRKE-8, was harvested either at logarithmic growth (L) or at confluency (C). Five (TRKE-5) or 10 μg (TRKE-4, -7, -8) of total RNA was hybridized to anti-sense Z5.9zf(−) in a RNase protection assay.

Expression of Kid-1 in kidney disease. After renal injury, Kid-1 mRNA levels decline rapidly and transiently (38) at a time when the surviving tubular cells dedifferentiate and divide (37). Kidney Kid-1 mRNA levels increase with time after birth and are highest in the adult rat (38). These findings suggest that transcription of the *Kid*-1 gene and/or the stability of the transcript are decreased in cells that are less differentiated. The expression pattern of the Kid-1 protein during nephron development is consistent with this concept. In addition, our results with polycystic kidneys, renal cell carcinomas, and immortal rat kidney epithelial cell lines lend more support to this hypothesis. Both polycystic kidneys and renal cell carcinomas are characterized by a lower degree of cellular differentiation, higher mitotic rates, and lower Kid-1 mRNA levels than the adult normal kidney. It is interesting that in the polycystic kidneys of heterozygous female Han:SPRD (*cy*/+) rats, in which the polycystic phenotype is milder than in male (*cy*/+) rats (14), the mRNA levels of Kid-1 are the same as in age-matched, wild-type animals.

Similar to human autosomal dominant PKD, only a subset of nephrons in the Han:SPRD (*cy*/+) rat become cystically dilated (26). Thus Northern blot analysis, in which total kidney RNA is examined, underestimates the marked decrease of Kid-1 protein expression in cyst-lining cells demonstrated by immunohistochemical staining. The loss of Kid-1 protein expression occurred in the same cells in which there was loss of alkaline phosphatase activity, which is consistent with the appearance of Kid-1 late during nephron development when the epithelial cells are more differentiated. During nephron development, Kid-1 protein appears approximately at the same time as alkaline phosphatase activity; in cyst wall epithelia, Kid-1 disappears after or at the same time as the loss of alkaline phosphatase. Dedifferentiation in cyst wall cells in kidneys from the Han:SPRD (*cy*/+) rat likely is a graded process and appears first to be associated with a loss of expression of alkaline phosphatase and decrease in Kid-1 protein, followed by further loss of the Kid-1 protein.

The pattern of Kid-1 mRNA expression in polycystic kidneys is not specific to the Han:SPRD (*cy*/+) rat model of autosomal dominant PKD, because a similar pattern can be seen in polycystic kidneys from the

C57BL/6J (*cpk*/*cpk*) mouse, a model for autosomal recessive PKD. Kid-1 mRNA levels were much lower in kidneys from homozygous (*cpk*/*cpk*) mice than in kidneys from control animals of the same age. The affected gene in Han:SPRD rats is located on rat chromosome 5 (2), whereas in the (*cpk*/*cpk*) model the affected gene lies on mouse chromosome 12 (10). Both loci are different from the locus of the *Kid*-1 gene [chromosome 10 in the rat (40) and chromosome 11 in the mouse (32)], so that a mutation in the *Kid*-1 gene cannot be the cause of the disease in either animal model. It is possible that the decrease of Kid-1 expression contributes to a pattern of epithelial dedifferentiation common to both models. Because Kid-1 is a transcriptional repressor, it is likely that a regulated gene is repressed when Kid-1 is expressed. When Kid-1 expression is suppressed there may be enhanced production of a protein, which then may contribute to the cystic phenotype.

In transformed epithelial cell lines from the rat kidney, mRNA levels of Kid-1 are low. This observation is consistent with the hypothesis that rapidly dividing and dedifferentiated cells have downregulated the expression of Kid-1. We could, however, see no difference between cells in a logarithmic growth state or at confluency. The mechanisms, however, by which growth arrest and differentiation are brought about probably share certain features, but also are different in other aspects. Growing these cell lines to confluence may not have been sufficient to achieve a level of differentiation associated with increases in Kid-1 mRNA levels.

In summary, Kid-1 is expressed prominently in the proximal tubule. Levels of Kid-1 increase during nephron development and are markedly reduced in two animal models of PKD, in rat renal cell carcinomas, and in TRKE cell lines. Each of the latter conditions is characterized by a proliferative phenotype with a low level of differentiation. We propose that this decreased Kid-1 expression may contribute to the derepression of genes, which in turn may contribute to the abnormal cyst phenotype of PKD and perhaps the dedifferentiated and highly proliferative state of renal tumor cells and transformed cell lines.

We acknowledge the skillful introduction to hybridoma technology by Peter Mundel and the kind gifts of materials from Jack Dixon (pGEX-KG) and John Kyriakis (pMT3), without which this work would not have been possible. Michael Kramer kindly established the isotype of the hybridoma 5D12. The expert photographic work of Ingrid Ertel and graphics of Rolf Nonnenmacher are gratefully acknowledged. We also thank Karen Dellovo and Alessandro Alessandrini for help with the figures.

The experiments described were made possible by financial support from the Deutsche Forschungsgemeinschaft to R. Witzgall (Wi 1042/2–1 and Wi 1042/2–2) and National Institutes of Health MERIT Award DK-39773 to J. V. Bonventre.

Address for reprint requests: R. Witzgall, University of Heidelberg, Institute of Anatomy and Cell Biology I, Im Neuenheimer Feld 307, 69120 Heidelberg, Germany.

Received 13 March 1998; accepted in final form 3 September 1998.

REFERENCES

1. **Ausubel, F. M., R. Brent, R. E. Kingston, D. D. Moore, J. G. Seidman, J. A. Smith, and K. Struhl.** *Current Protocols in Molecular Biology*. New York: Wiley, 1996.
2. **Bihoreau, M. T., I. Ceccherini, J. Browne, B. Kränzlin, G. Romeo, G. M. Lathrop, M. R. James, and N. Gretz.** Location of the first genetic locus, PKDr1, controlling autosomal dominant polycystic kidney disease in Han:SPRD *cy*/+ rat. *Hum. Mol. Genet*. 6: 609–613, 1997.
3. **Brady, J. P., M. K. Duncan, E. F. Wawrousek, and J. Piatigorsky.** The transcription factor, Kid-1, is highly expressed in both eye and kidney of the mouse. *Exp. Eye Res*. 64: 287–290, 1997.
4. **Calvet, J. P.** Polycystic kidney disease: primary extracellular matrix abnormality or defective cellular differentiation? *Kidney Int*. 43: 101–108, 1993.
5. **Chailler, P., and N. Brière.** Integration of proliferation and differentiation phenomena during rodent kidney ontogeny. *Growth Dev. Aging* 55: 11–18, 1991.
6. **Chomczynski, P., and N. Sacchi.** Single-step method of RNA isolation by acid guanidinium thiocyanate-phenol-chloroform extraction. *Anal. Biochem*. 162: 156–159, 1987.
7. **Chong, J. A., J. Tapia-Ramirez, J. Kim, J. J. Toledo-Aral, Y. Zheng, M. C. Boutros, Y. M. Altshuller, M. A. Frohman, S. D. Kraner, and G. Mandel.** REST: a mammalian silencer protein that restricts sodium channel gene expression to neurons. *Cell* 80: 949–957, 1995.
8. **Cowley, Jr., B. D., L. J. Chadwick, J. J. Grantham, and J. P. Calvet.** Elevated proto-oncogene expression in polycystic kidneys of the C57BL/6J (*cpk*) mouse. *J. Am. Soc. Nephrol*. 1: 1048–1053, 1991.
9. **Cowley, Jr., B. D., S. Gudapaty, A. L. Kraybill, B. D. Barash, M. A. Harding, J. P. Calvet, and V. H. Gattone.** Autosomal-dominant polycystic kidney disease in the rat. *Kidney Int*. 43: 522–534, 1993.
10. **Davisson, M. T., L. M. Guay-Woodford, H. W. Harris, and P. D'Eustachi.** The mouse polycystic kidney disease mutation (cpk) is located on proximal chromosome 12. *Genomics* 9: 778–781, 1991.
11. **Eker, R., and J. Mossige.** A dominant gene for renal adenomas in the rat. *Nature* 189: 858–859, 1961.
12. **Fry, Jr., J. L., W. E. Koch, C. Jennette, E. McFarland, F. A. Fried, and J. Mandell.** A genetically determined murine model of infantile polycystic kidney disease. *J. Urol*. 134: 828–833, 1985.
13. **Gattone, V. H., II, J. P. Calvet, B. D. Cowley, Jr., A. P. Evan, T. S. Shaver, K. Helmstadter, and J. J. Grantham.** Autosomal recessive polycystic kidney disease in a murine model. A gross and microscopic description. *Lab. Invest*. 59: 231–238, 1988.
14. **Gretz, N., I. Ceccherini, B. Kranzlin, I. Kloting, M. Devoto, P. Rohmeiss, B. Hocher, R. Waldherr, and G. Romeo.** Gender-dependent disease severity in autosomal polycystic kidney disease of rats. *Kidney Int*. 48: 496–500, 1995.
15. **Guan, K. L., and J. E. Dixon.** Eukaryotic proteins expressed in *Escherichia coli*: an improved thrombin cleavage and purification procedure of fusion proteins with glutathione *S*-transferase. *Anal. Biochem*. 192: 262–267, 1991.
16. **Hatini, V., S. O. Huh, D. Herzlinger, V. C. Soares, and E. Lai.** Essential role of stromal mesenchyme in kidney morphogenesis revealed by targeted disruption of Winged Helix transcription factor *BF-2*. *Genes Dev*. 10: 1467–1478, 1996.
17. **Hoppe-Seyler, F., K. Butz, C. Rittmuller, and M. von Knebel Doeberitz.** A rapid microscale procedure for the simultaneous preparation of cytoplasmic RNA, nuclear DNA binding proteins and enzymatically active luciferase extracts. *Nucleic Acids Res*. 19: 5080, 1991.
18. **Kaufman, R. J.** Vectors used for expression in mammalian cells. *Methods Enzymol*. 185: 487–511, 1990.
19. **Knapek, D. F., M. Serrano, D. Beach, D. Trono, and C. L. Walker.** Association of rat $p15^{INK4B}$/$p16^{INK4}$ deletions with monosomy 5 in kidney epithelial cell lines but not primary renal tumors. *Cancer Res*. 55: 1607–1612, 1995.
20. **Kobayashi, T., Y. Hirayama, E. Kobayashi, Y. Kubo, and O. Hino.** A germline mutation in the tuberous sclerosis (*Tsc2*) gene gives rise to the Eker rat model of dominantly inherited cancer. *Nat. Genet*. 9: 70–74, 1995.

21. **Kreidberg, J. A., H. Sariola, J. M. Loring, M. Maeda, J. Pelletier, D. Housman, and R. Jaenisch.** WT-1 is required for early kidney development. *Cell* 74: 679–691, 1993.
22. **Larsson, L.** The ultrastructure of the developing proximal tubule in the rat kidney. *J. Ultrastruct. Res.* 51: 119–131, 1975.
23. **Margolin, J. F., J. R. Friedman, W. K.-H. Meyer, H. Vissing, H.-J. Thiesen, and F. J. Rauscher III.** Krüppel-associated boxes are potent transcriptional repression domains. *Proc. Natl. Acad. Sci. USA* 91: 4509–4513, 1994.
24. **Miyamoto, N., M. Yoshida, S. Kuratani, I. Matsuo, and S. Aizawa.** Defects of urogenital development in mice lacking Emx2. *Development* 124: 1653–1664, 1997.
25. **Moser, M., J. Ruschoff, and R. Buettner.** Comparative analysis of AP-2 alpha and AP-2 beta gene expression during murine embryogenesis. *Dev. Dyn*. 208: 115–124, 1997.
26. **Obermüller, N., N. Gretz, W. Kriz, F. J. van der Woude, R. F. Reilly, H. Murer, J. Biber, and R. Witzgall.** Differentiation and cell polarity during renal cyst formation in the Han:SPRD (*cy*/+) rat, a model for ADPKD. *Am. J. Physiol*. 273 (*Renal Physiol*. 42): F357–F371, 1997.
27. **Pontoglio, M., J. Barra, M. Hadchouel, A. Doyen, C. Kress, J. P. Bach, C. Babinet, and M. Yaniv.** Hepatocyte nuclear factor 1 inactivation results in hepatic dysfunction, phenylketonuria, and renal Fanconi syndrome. *Cell* 84: 575–585, 1996.
28. **Preminger, G. M., W. E. Koch, F. A. Fried, E. McFarland, E. D. Murphy, and J. Mandell.** Murine congenital polycystic kidney disease: a model for studying development of cystic disease. *J. Urol*. 127: 556–560, 1982.
29. **Saxén, L.** *Organogenesis of the Kidney*, edited by P. Barlow, P. Green, and C. Wylie. Cambridge, UK: Cambridge University Press, 1987. (Dev. Cell Biol. Ser. 19)
30. **Schäfer, K., N. Gretz, M. Bader, I. Oberbäumer, K.-U. Eckardt, W. Kriz, and S. Bachmann.** Characterization of the Han:SPRD rat model for hereditary polycystic kidney disease. *Kidney Int*. 46: 134–152, 1994.
31. **Schoenherr, C. J., and D. J. Anderson.** The neuron-restrictive silencer factor (NRSF): a coordinate repressor of multiple neuron-specific genes. *Science* 267: 1360–1363, 1995.
32. **Sornson, M. W., W. Wu, J. S. Dasen, S. E. Flynn, D. J. Norman, S. M. O'Connell, I. Gukovsky, C. Carrière, A. K. Ryan, A. P. Miller, L. Zuo, A. S. Gleiberman, B. Andersen, W. G. Beamer, and M. G. Rosenfeld.** Pituitary lineage determination by the *Prophet of Pit-1* homeodomain factor defective in Ames dwarfism. *Nature* 384: 327–332, 1996.
33. **Sturzl, M., and W. K. Roth.** "Run-off" synthesis and application of defined single-stranded DNA hybridization probes. *Anal. Biochem*. 185: 164–169, 1990.
34. **Torres, M., E. Gómez-Pardo, G. R. Dressler, and P. Gruss.** *Pax*-2 controls multiple steps of urogenital development. *Development* 121: 4057–4065, 1995.
35. **Walker, C., and J. Ginsler.** Development of a quantitative in vitro transformation assay for kidney epithelial cells. *Carcinogenesis* 13: 25–32, 1992.
36. **Walker, C., T. L. Goldsworthy, D. C. Wolf, and J. Everitt.** Predisposition to renal cell carcinoma due to alteration of a cancer susceptibility gene. *Science* 255: 1693–1695, 1992.
37. **Witzgall, R., D. Brown, C. Schwarz, and J. V. Bonventre.** Localization of proliferating cell nuclear antigen, vimentin, c-*fos*, and clusterin in the post-ischemic kidney. Evidence for a heterogeneous genetic response among nephron segments, and a large pool of mitotically active and dedifferentiated cells. *J. Clin. Invest*. 93: 2175–2188, 1994.
38. **Witzgall, R., E. O'Leary, R. Gessner, A. J. Ouellette, and J. V. Bonventre.** *Kid-1*, a putative renal transcription factor: regulation during ontogeny, and in response to ischemia and toxic injury. *Mol. Cell. Biol*. 13: 1933–1942, 1993.
39. **Witzgall, R., E. O'Leary, A. Leaf, D. Önaldi, and J. V. Bonventre.** The Krüppel-associated box-A (KRAB-A) domain of zinc finger proteins mediates transcriptional repression. *Proc. Natl. Acad. Sci. USA* 91: 4514–4518, 1994.
40. **Witzgall, R., R. Volk, R. S. Yeung, and J. V. Bonventre.** Genomic structure and chromosomal location of the rat gene encoding the zinc finger transcription factor Kid-1. *Genomics* 20: 203–209, 1994.
41. **Yeung, R. S., G.-H. Xiao, F. Jin, W.-C. Lee, J. R. Testa, and A. G. Knudson.** Predisposition to renal carcinoma in the Eker rat is determined by germ-line mutation of the tuberous sclerosis 2 (TSC2) gene. *Proc. Natl. Acad. Sci. USA* 91: 11413–11416, 1994.